⊙ Technical Paper

Design Guidelines of Elevated Buildings for Antarctic Environment (I)-Wind Load

D.H.Kim*, K.C.S. Kwok** and H.F. Rohde***

(*Received December* 3, 1990)

南極環境을 위한 高床式 建物의 Design Guideline에 관한 硏究(I)-風何重

金 東 潕* · K.C.S. Kwok** · H.F. Rohde***

Key Words : Antarctic Building(南極建物), Snowdrifting(積雪現象), Wind Load(風何重), Boundary Layer Wind Tunnel(境界層難流風洞), Elevated Building(高床式建物)

抄 錄

南極建物은 南極의 거센 바람 및 이에 수반되는 積雪現象을 피하기 위해 땅에서 띄우는 高床式 및 地下에 設置하는, 두가지의 形態를 취하고 있다. 高床式의 경우 建物밑으로 바람을 通하게 함으로써 積雪現象을 피하는데 効果的이기는 하나 南極의 거센 바람에 對應하기 위하여 構造的인 問題를 해결해야 하는 취약점을 지니고 있다. 本 硏究는 境界層難流風洞을 利用하여 高床式 南極建物에 가해지는 風何重을 把握함으로서 南極建物의 design guideline을 提示하였다.

1. Introduction

Following the progressive obliteration of several stations in Antarctica by snowdrifting, two alternative remedies were explored, viz. underground and elevated structures (Radok, 1977). Elevation of structures has been a popular method because of its effectiveness in minimising snowdrifiting accumulation around buildings by allowing the wind to sweep through beneath the buildings and because of its convenience of construction. This method only works if the slot under the building is big enough and resonably free from obstructions. However this approach increases the structural requirements for strength and rigidity

* Member, Research Associate, School of Civil and Mining Engineering, The University of Sydney, N.S.W. 2006, Australia

** Associate Professor, School of Civil and Mining Engineering, The University of Sydney, N.S.W. 2006, Australia

*** Managing Partner, Helmut Rohde and Partners, 1 Hosking St., Balmain East, N.S.W. 2041, Australia

and also creates a freezing wind flow underneath the floor of the building.

Australia's old Casey station is an example. The station was especially designed to counteract the problem of snowdrifting. Although the design was effective in its primary objective of minimising snowdrifting accumulation, it was found to have some undesirable features. As an elevated structure (ranging from 5 to 11 feet above ground), it developed structural vibration problems under wind speeds of up to 300 *km/h*. It rattled and shaked (Incoll, 1990). Access was more difficult due to its height above ground, particularly for carrying heavy items. The occupants of the building were subject to noise and vibration which accentuated their impression of the severity of the weather conditions outside and apparently increased their reluctance to go outside. It was reported that morale at old Casey station was lower and less work was done than other stations (Gosbell and Holmes, 1982). This example suggests that snowdrifting clearance should not be investigated in isolation from structural vibration and wind loading. It is also believed that the building shape facing wind and the height above ground appear to be the major design factor in terms of wind loading on Antarctic buildings.

This paper describes measurements of the wind loads on seven 1/50 scale models with differenct corner geometries, heights above ground and incident wind angles in a wind tunnel with properly simulated atmospheric turbulent boundary layer flow, prior to investigating the snowdrifting accumulation. A 1/50 scale boundary layer wind model over a terrain category 2 (Australian Standard, AS 1170.2—1989), which may represent summer condition of coastal sites of Australian Antarctic Territory (Kim et al, 1990), was generated in the No. 1 open-circuit Boundary Layer Wind Tunnel (No. 1 B.L.W.T.). A force balance was used to measure the horizontal and vertical forces on the models. Coefficients of mean drag, mean lift, standard deviation of drag and lift of the models were obtained.

2. Background

There has been tremendous growth in research and testing activities in the field of wind engineering during the past twenty years. In the case of Antarctic buildings, wind has to be regarded as one of the important design factor since Antarctica is one of the windiest continents on Earth.

The study of wind loads on low rise buildings using either full-scale or wind tunnel model tests is a relatively new area. Only recently attention has been given to fluctuating wind effects on low-rise buildings. Eaton and Mayne (1975) performed full-scale measurements on a two-storey house at Aylebury. Eaton et al (1975) and Best and Holmes (1978) investigated the effect of roof geometry on wind loads on low-rise buildings. Stathopoulos (1984), and Kim and Mehta (1977) investigated the wind loads on flat roof surfaces. Marshall (1977) also conducted full-scale measurement of wind loads on a mobile home. Davenport et al. (1977, 1978) and Surry et al (1978) investigated wind loads on low-rise buildings. Holmes (1980) reported wind pressures and forces on tropical houses. Best and Holmes (1978) performed a wind tunnel model study of wind presssures on an isolated single-storey house. Roy (1983) perfo-rmed wind tunnel measurement of wind loads on a mobile home by using a force balance system and compared the results with full-scale measurements done by Marshall (1977). Holmes and Best (1981) investigated wind effects by using a covariance integration technique to predict total loads on a bay section of a low-rise building.

The above studies were all based on isolated buildings in an open terrain. However, to the best of the author's knowledge, a systematic study of

the wind loads on elevated buildings with various corner geometries has not been performed, and certainly not for Antarctic conditions. Therefore, it was believed that a wind tunnel model study was needed to investigate the relationships between wind loads, height above ground, incident wind angles and corner geometries. The results of these tests could lead to wind loading desing guidelines for Antarctic buildings.

3. Wind Tunnel Models

The models used were based on dimensions of 120 *mm* × 56 *mm* × 72 *mm*, representing a model of 1 50 scale module similar to a shipping container. In order to achieve a high natural frequency, lightweight rigid materials were considered. Extruded polystyrene provided suitable rigidity and density. Seven different shapes were made and given a smooth surface finish. Details of their dimensions and shapes are given in Table 1.

Model 1, which was a plain rectangular shape, was used as a reference model. Models 2, 3, and 4 have all edges chamfered by 45 degree to equivalent prototype scale depths of 400 *mm*, 600 *mm*, and 800 *mm* respectively in prototype. Models 5, 6, and 7 have all edges radiused by 400 *mm*, 600 *mm*, and 800 *mm* respectively.

4. Modelling of the Turbulent Boundary Layer Flow

4. 1 Reynolds number

One of the most common deficiencies in wind tunnel model test is the inability to achieve a high Reynolds number flow comparable to the full scale supercritical Reynolds number flow situation. In real flow, the magnitude of the shearing stress between fluid layers is significant and the fluid density may vary, although for the velocities under consideration the density remains essentially constant. The flow field or pattern of flow around a circular cross-section in real flow varies, depending on the ratio of the shearing stress to the dynamic pressure of the flow. This ratio is

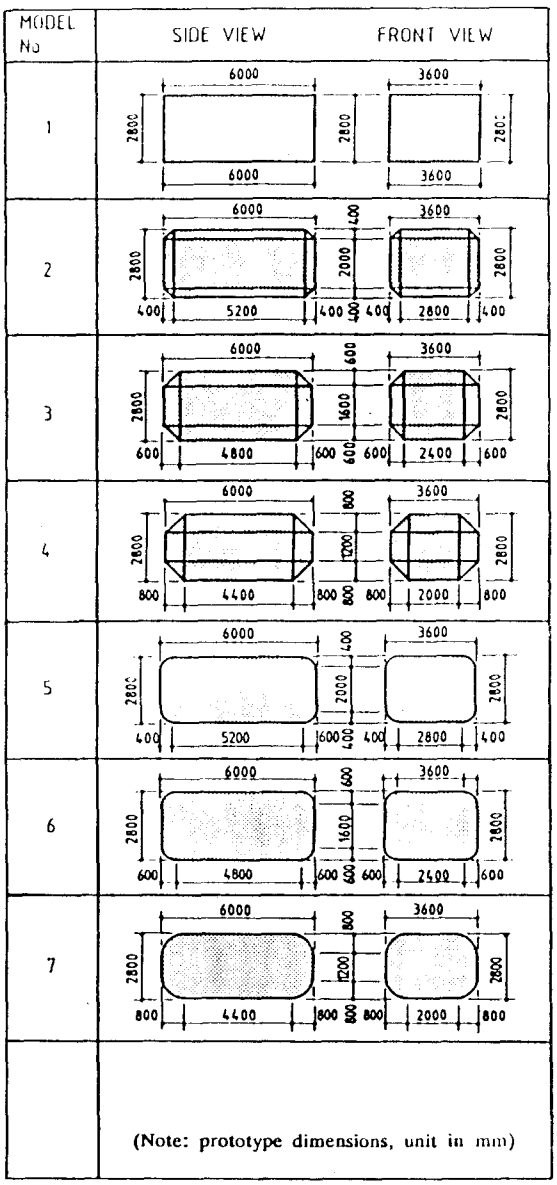

Table 1 Detailed dimensions of wind tunnel models

known as the Reynolds number, which can be expressed as follows :

$$Re = \frac{u\,d}{\nu} \quad \cdots\cdots (5)$$

in which u is the mean wind velocity, d is the diameter of the circular shape and ν is the kinematic viscosity of air.

Fortunately most structures have sharp edges and the wind distribution and force characteristics of these structures appear to be relatively independent of Reynolds number, so that errors due to incorrect scaling are small. However, for structures with circular features, the flow field around the structures and the resultant wind forces can be sensitive to the Reynolds number of the flow. Therefore, results of model tests of this type of structures must be treated with caution.

By restricting attention to Reynolds numbers larger than 1×10^4, the flow around a circular cylinder can be divided into a number of flow regimes, each with distinct boundary layer behaviour, Strouhal number, pressure distribution and drag force characteristics (Kwok, 1985). As was first suggested by Roshko (1961), and recently proposed by Farell (1981, 1983), and ESDU 80025 (1980), at least three flow regimes can be identified : subcritical (having a Reynolds number of up to about 10^5), supercritical and transcritical (which begins at a Reynolds number of the order of 10^6), with a lower transition separating the subcritical and supercritical regimes and an upper transition separating the supercritical and transcritical regimes.

It has also been noted that the lower transition is marked by a decrease in the drag coefficient from about 1.15 at a Reynolds number of about 1.5×10^5 to about 0.25 at a Reynolds number of about 4×10^5(Kwok, 1985). The formation of laminar-separation-turbulent-reattachment bubbles (Achenbach, 1971 and Bearman, 1968) is believed to be responsible for the lowered value of the drag coefficient which signifies the beginning of the supercritical flow regime.

However many researchers agree that the supercritical region can be accepted as a Reynolds-number-Independent region, even though the drag does marginally indcrease with Reynolds number (e.g. Macdonald, 1987). Roshiko (1961) also noted that, in the transcritical region, Reynolds number has no apparent effect on the drag coefficient.

It is often difficult to simulate high Reynolds number flow conditions because of limitations imposed by model size. Cheung and Melbourne (1983) recently indicated that model tests with circular features can be performed satisfactorily provided the test Reynolds number in a turbulent flow with turbulence intensity greater than 4%, is in excess of 2×10^5. It was further concluded that model tests with a Reynolds number below 2×10^5 have little relevance to the full scale situation and results obtained from such tests are virtually useless. Macdonald (1987) performed a series of tests to investigate the sensitivity of the mean pressure distribution around isolated silos to variations in Reynolds number. It was suggested that the mean wall pressure distribution is independent of Reynolds number if the test Reynolds number exceeds about 1×10^5 in a turbulent boundary layer flow. Results of recent works (Mulhearn et al, 1976 ; Finnigan and Longstaff, 1982) support this lower limit for Reynolds number independence.

Taking the model with the smallest corner radius of 8 *mm*(400 *mm* in prototype) used in this study, the model test Reynolds number would be approximately 1×10^4 in the wind tunnel. Since the above Reynolds numbers were within the range of subcritical flow, the Reynolds number was effectively increased by adding moderate surface roughness to the model, and by considering the

turbulence intensity of the approaching flow. ESDU 80025 (1980) provides a method for the estimatimation of an effective Reynolds number $Re_e(=\lambda_T \lambda_R Re)$, which is a modified Reynolds number incorporating the factors λ_T (dependent on the turbulence characteristics of the approaching flow) and λ_R (dependent on the surface roughness parameter). Since the measured mean effective surface roughness height of the model is appominately $5\times10^{-5}m$, λ_R is estimated to be approximately 3, according to the data provided by ESDU (1980). Also the values of λ_T are approximately 5. 52 (from ESDU 80025, 1980). Hence the value of Re_e was estimated to be 1.7×10^5.

Although the above value of $Re_e(=1.7\times10^5)$ is slightly lower than the suggested value (ESDU 80025, 1980) for supercritical flow ($Re > 3\times10^5$) and the value of 2×10^5 suggested by Cheung and Melbourne (1983), it is within the range of the value suggested by Macdonald (1987). Therefore, Reynolds number problem can be ignored in this study.

4. 2 Turbulent Boundary Layer Wind

Similarity between the model and prototype values of following parameters is considered to be the minimum requirement for the satisfactory simulation of an atmospheric turbulent boundary layer flow :

(1) mean wind velocity profile ;
(2) turbulence intensity profiles ;
(3) Reynolds stress profile ; and
(4) turbulence length scale and spectrum

An open flat terrain (a terrain category type 2, AS 1170.2－1989) was adopted as the prototype summer condition in this investigation. Wind tunnel tests were carried out in the testing section ($2.0m$ high by $2.4m$ wide) of the No.1 B.L.W.T., which is shown in Figure 1. To generate the turbulent boundary layer flow, a $300mm$ high tripboard was installed at the start of the working section, and the floor of the working section was covered with low-pile carpet.

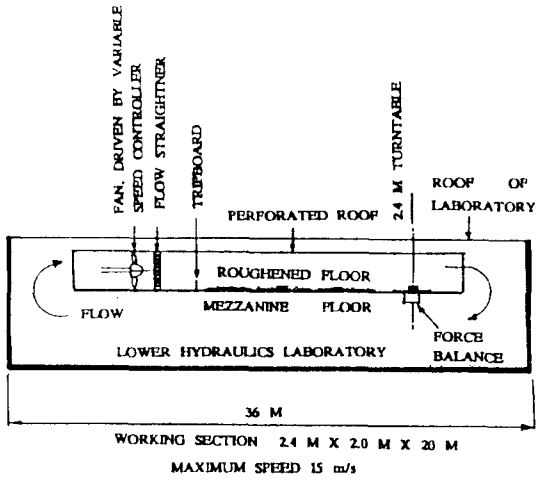

Fig. 1 Arrangement of No.1 Turbulent boundary layer wind tunnel, School of Civil and Mining Engineering, the University of Sydney

The flow characteristics of the simulated atmospheric boundary layer were measured at $15m$ downstream from the tripboard at three lateral position : at the centre of the working section, and $0.6m$ from the centre on either side. The Mean wind speed at the reference height ($10m$ in prototype) was approximately $10m/s$. A hot wire anemometer was used to measure the profiles of mean wind speed and longitudinal turbulence intensity, and the longitudinal turbulence spectrum. Profiles from $25mm$ up to a height of $300mm$ above the tunnel floor were measured at each of the three lateral positions using the constant temperature anemometer. The signals from the hot wire anenometer were linearised, low-pass filtered and processed by a micro computer.

4. 2. 1 Mean Wind Velocity Profiles

The mean wind velocity profiles for the three lateral positions are presented in Figure 2, with

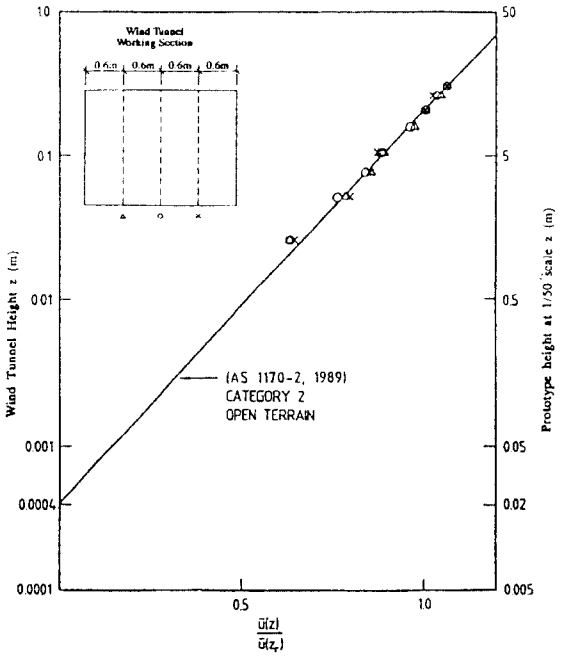

Fig. 2 Mean wind velocity profiles (Log-linear Format)

a logarithmic law with a roughness height of $z_0 = 0.02\,m$(prototype). They were compared with a profile suggested by AS 1170.2－1989 for comparision. A good agreement with the suggested profiles is evident.

4.2.2 Turbulence Intensity Profiles

Longitudinal, lateral and vertical turbulence intensity profiles are plotted in Figure 3. These turbulence intensity profiles are compared with profiles suggested by AS 1170.2 (1983, 1989) and showed a reasonably good agreement. At a height of $0.2\,m$($10\,m$ in prototype), the lateral turbulence intensity is about 85% of the longitudinal value, and the vertical turbulence intensity is about 55% of the longitudinal value. These values are consistent with those suggested in ESDU 74031(1974).

4.2.3 Reynolds Stress Profile

The measured Reynolds stress profile in the simulated boundary layer flow is nearly constant

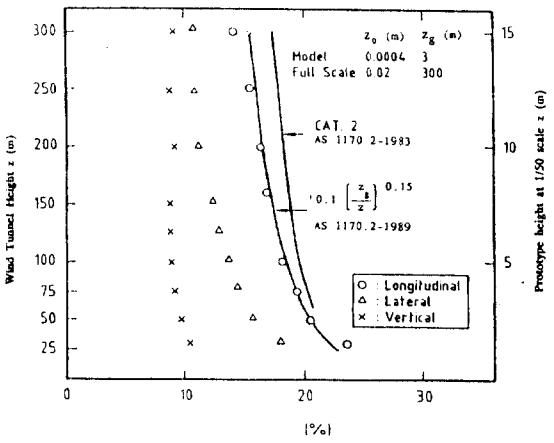

Fig. 3 Turbulence intensity profiles measured at the centre of the working section

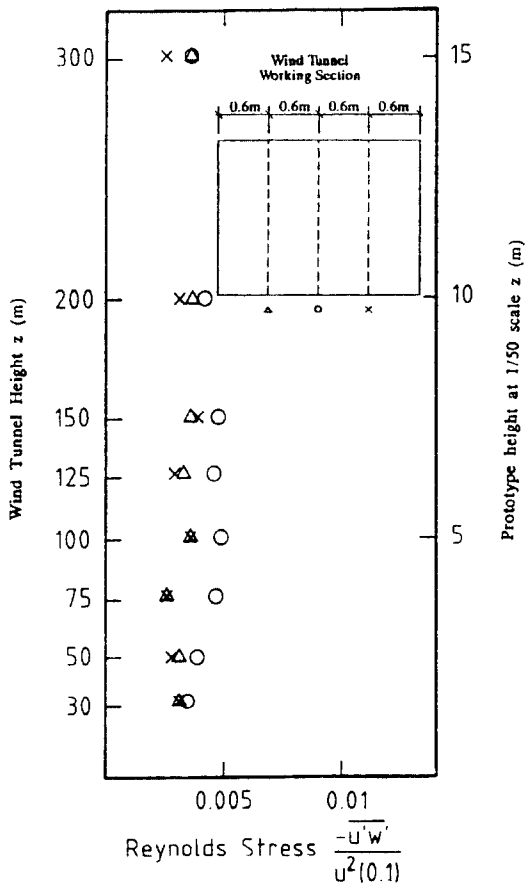

Fig. 4 Reynolds stress profiles

with height and is shown in Figure 4. The concentrated Reynolds stress which was expected to be present in the shear layer originating from the 0.3 m high tripboard fence has largely disappeared at the measuring point 15 *m* downstream from the fence.

4.4 Turbulence Length Scale and Spectrum

The longitudinal turbulence spectrum is used to determine the distribution of turbulence energy as a function of frequency, which gives a measured size of turbulence eddies. A velocity spectrum was measured at the wind tunnel centre line at a height of 200 *mm* (equivalent to 10 *m* in prototype) and plotted in Figure 5, where it is compared with ESDU 74031 (1974). For a nominal scale of 1/50, there is a reasonable good match.

5. Force Measurement

The wind-induced forces and responses of the buildings can be resolved into two orthogonal components for convenience. These forces and responses are parallel (drag) and perpendicular (lift) to the mean wind direction. For the practical application for engineering purpose, it is common

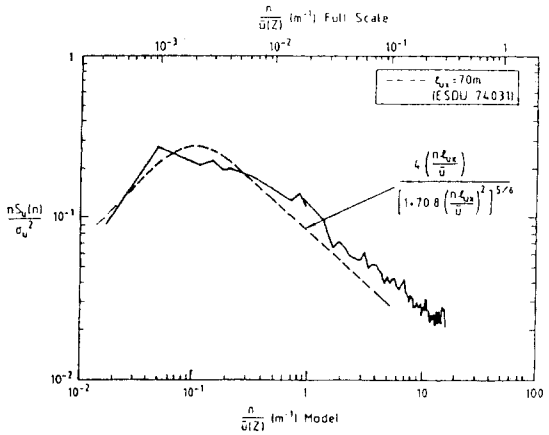

Fig. 5 Longitudinal turbulence spectrum at 1/50 scale

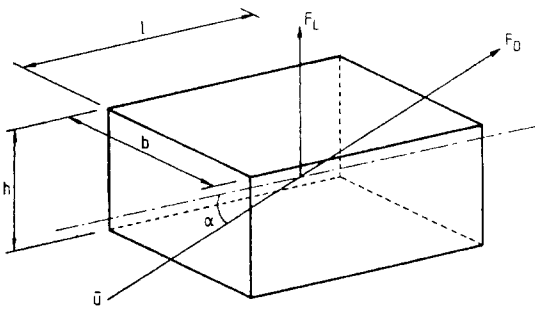

Fig. 6 Wind induced lift (F_L) and drag (F_D) on model

procedure to state the force into the components, i.e. F_x, F_y, and F_z. However, within the limited capabilities of apparatus, it was only possible to measure the along wind drag (F_D) and life (F_L) simultaneously, as shown in Figure 6. Therefore, this paper is concerned primarily with the identification of drag and lift forces on Antarctic building models with various corner geometries, incident wind angles, and heights above ground.

A force balance was installed at the centre of the wind tunnel working section, on which a building model was mounted. The model and balance responded with a resonant frequency of around 67 *Hz*. The signal output from the force transducer was low-pass filtered at 30 *Hz* to remove the resonant component of the signal and to attenuate the high instrumentation noise. By taking 17 *m/s* and 6 *m/s* as prototype maximum mean speed (Mitsuhashi, 1982) and testing mean wind velocity, respectively, frequency response of the balance and model equivalent was found to be 1.7 *Hz* in prototype which is believed to be appropriate to the generally accepted response of up to 1 *Hz* (prototype) for low rise building (Roy, 1983). The resulting signal was digitized by means of an analogue to digital converter, and sampled by a micro-computer. The response of the transducer was determined by calibration.

For each of the seven models, the wind lift and

drag were measured at seven different incident wind angles (0° to 90° at 15° intervals) and three different heights above ground (0.9 *m*, 1.2 *m*, and 1.5 *m* in prototype). Sample times of approximately 30 seconds were used and four samples were averaged for each of incident wind angles and heights above ground. This sampling period were equivalent to approximately 1 hour in prototype. The mean and standard deviation of drag and lift forces were measured and these were non-dimensionalised and expressed in the following form

: Mean drag coefficient

$$C_{FD} = \frac{F_D}{\frac{1}{2}\rho_a \bar{u}^2_{(h)} A_D} \quad \cdots\cdots (1)$$

Mean lift coefficient

$$C_{FL} = \frac{F_L}{\frac{1}{2}\rho_a \bar{u}^2_{(h)} A_L} \quad \cdots\cdots (2)$$

Standard deviation of drag coefficient

$$C_{FD}' = \frac{F_D'}{\frac{1}{2}\rho_a \bar{u}^2_{(h)} A_D} \quad \cdots\cdots (3)$$

Standard deviation of lift coefficient

$$C_{FL}' = \frac{F_L'}{\frac{1}{2}\rho_a \bar{u}^2_{(h)} A_L} \quad \cdots\cdots (4)$$

where F_D = mean drag force
F_L = mean lift force
F_D' = standard deviation of drag
F_L' = standard deviation of lift
A_D = building area on along wind drag (b×h)
A_L = building area on lift (b×l)
ρ_a = air density (1.2 kg/m^3)
$\bar{u}_{(h)}$ = mean wind speed at building roof height

Calculation of drag and lift coefficients were based on A_D and A_L, respectively. Therefore C_{FD} is influenced by change in the incident wind angle, while C_{FL} is not.

6. Results of Force Coefficient Measurements

Figure 7 shows the effect of variation of height above ground on C_{FD} at $\alpha=0°$. h_1 is a height of

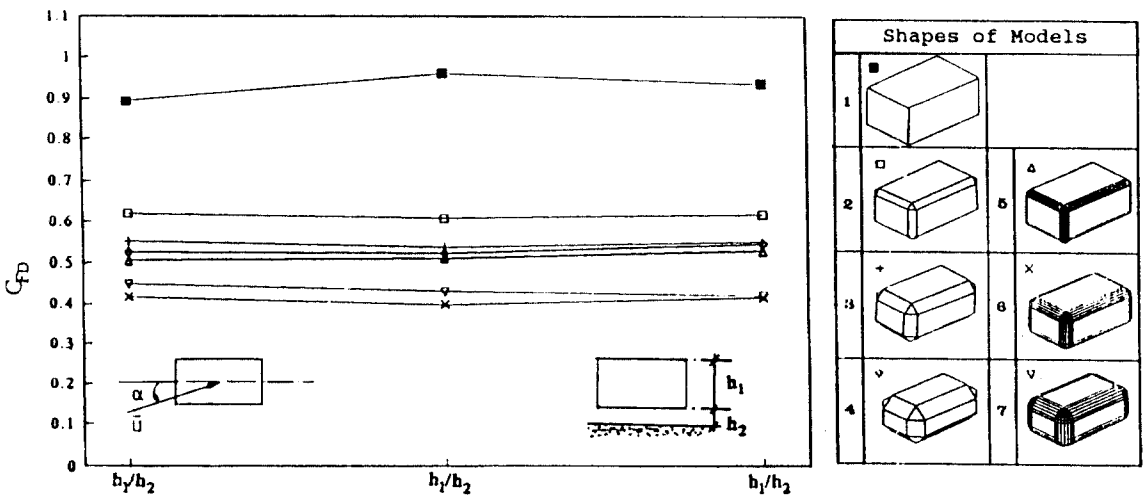

Fig. 7 C_{FD} at $\alpha=0°$ for different heights above ground

the model and h_2 is a height from the ground to the bottom of the model. It was found that, in general, the building height above ground did not have much effect on the force coefficients. A similar pattern of C_{FL}, C_{FD}' and C_{FL}' at $\alpha=0$ was observed for different building heights above ground (for more detail, refer to Kim et al, 1990).

Figures 8 to 11 show the effects of the different incident wind angles on the force coefficients at $h_1/h_2=3.1$. In general, the lift and drag force coefficients decrease with increasing chamfer or radius. Figure 8 shows that chamfered or radiused corner geometries caused reductions in the mean drag coefficient ranging from approximately 9% (Model No.2 at $\alpha=15^\circ$) to approximately 53% (Model No.6 at $\alpha=0^\circ$) compared with the reference model. Model No.7, wihich has the most radiused corner geometry, gave the largest reduction of C_{FS} at all incident wind angles, except at $\alpha=0^\circ$. A similar pattern was observed for C_{FD}' and C_{FL} as shown in Figures 9 and 10, respectively. Figure 11 shows that, in the case of C_{FL}', the

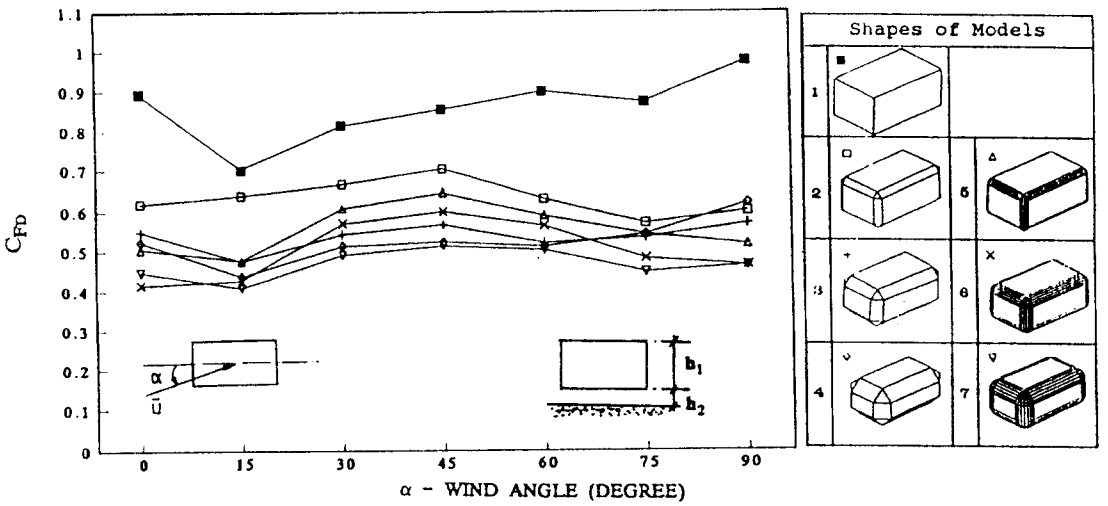

Fig. 8 C_{FD} at $h_1/h_2=3.1$ configuration

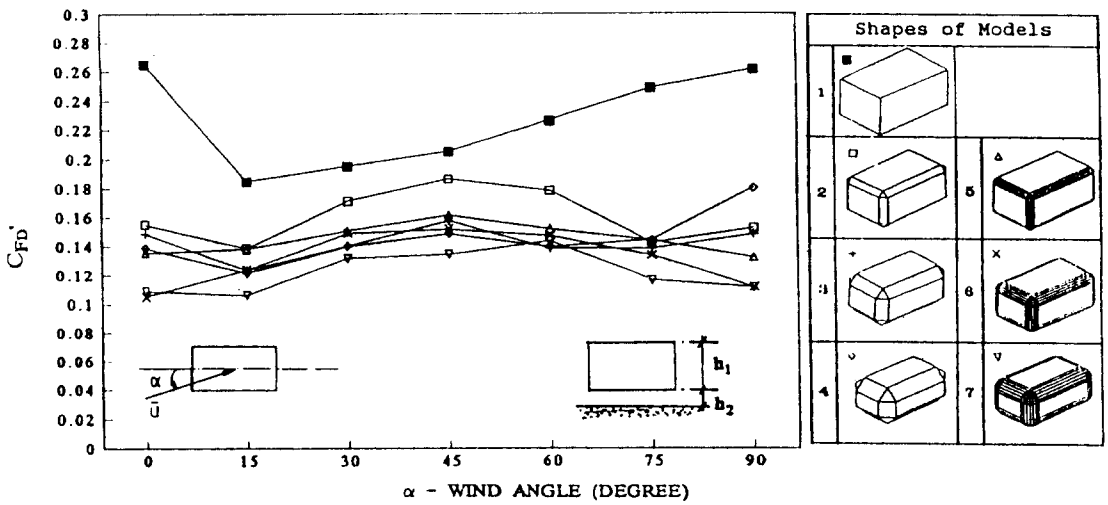

Fig. 9 C_{FD}' at $h_1/h_2=3.1$ configuration

largest reduction was observed at $\alpha=75°$ and $90°$ for Model No.7, with reduction of approximately 45% at both incident wind angles. However, Model No.4, which has the most chamfered corner geometry, gave the largest reduction of C_{FL}' at the other incident wind angles.

Figure 8 also shows that the maximum value of C_{FD} for Models 1, 3 and 4 occurred at the $\alpha=90°$, while the other configurations showed a maximum value of C_{FD} at $\alpha=45°$. Model Nos. 3 and 4 showed a steady rise in growth of values from $\alpha=45°$ up to $\alpha=90°$. A similar pattern was observed for C_{FD}', as shown in Figure 12. For C_{FL} and C_{FL}', the coefficients increased gradually up to their maximum values at $\alpha=90°$, as shown in Figures 10 and 11, respectively.

Similar relationships exist between force coefficients and different incident wind angles at the other model heights. For more detailed information, refer to Kim et al (1990).

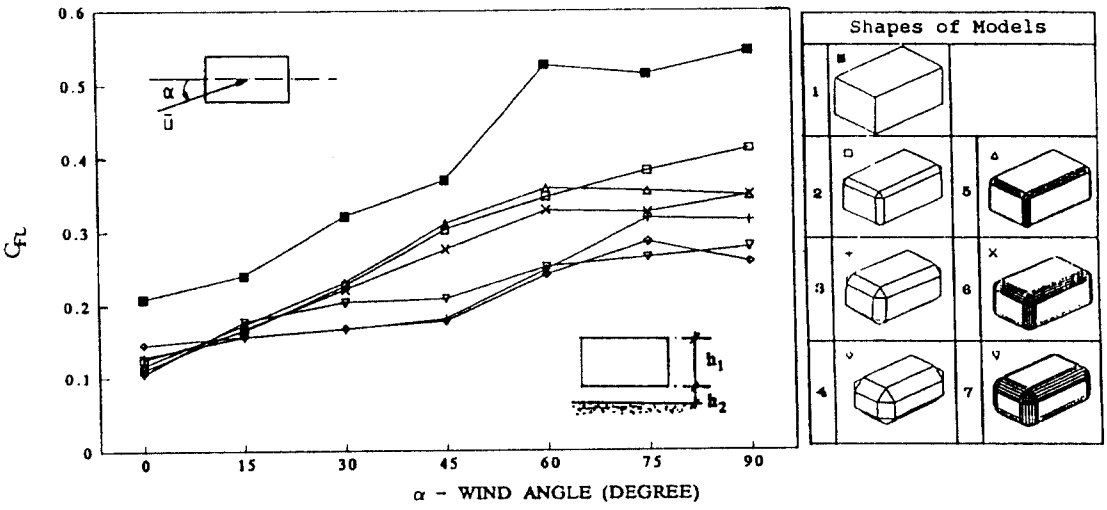

Fig. 10 C_{FL} at $h_1/h_2=3.1$ configuration

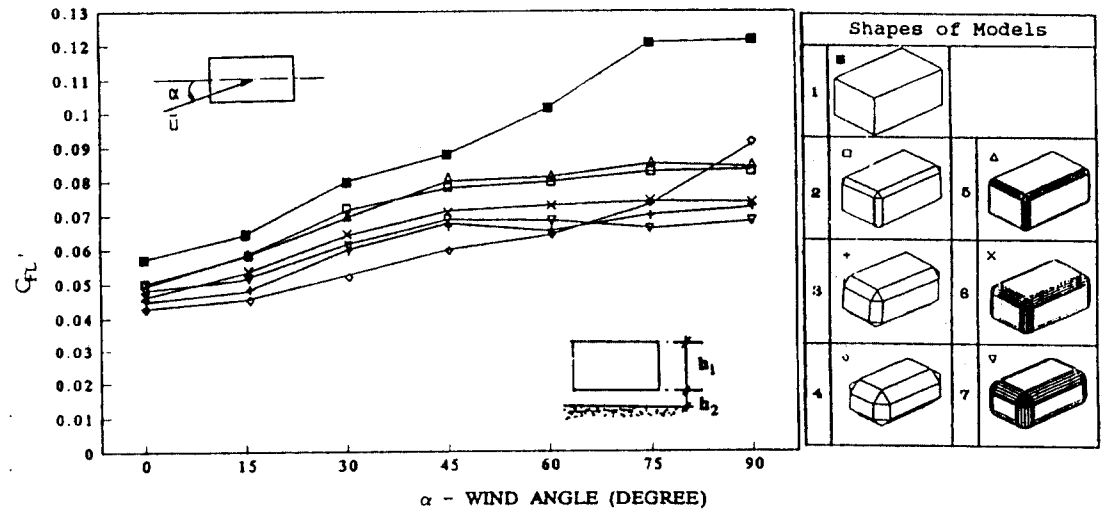

Fig. 11 C_{FL} at $h_1/h_2=3.1$ configuration

7. Conclusions and Recommendations

The main findings from this chapter of wind loads on elevated Antarctic buildings with different shapes, and at different wind directions and heights from the ground, are as follows :

1) A boundary layer flow (terrain category type 2, AS 1170, 2-1989) was generated to simulate the summer conditions at the coastal sites of Australian Antarctic Territory at a scale of 1/50 in the open-circuit Boundary Layer Wind tunnel. The use of a 300 *mm* high tripboard and low-pile carpet provided satisfactory simulation of the mean wind speed, turbulence intensity, Reynolds stress, and longitudinal turbulence spectrum profiles.

2) The test results showed that models with chamfered and rounded corners gave a reduction in wind loads in comparison to the rederence model, which was of a simple rectangular shape. It was also observed that the buildings with radiused corner geometry gave lower force coefficients than those with chamfered corner geometry.

These wind turnnel test results strongly indicate that elevated Antarctic buildings should have chamfered or radiused corners to reduce both the mean and fluctuating wind loads. The chamfer or radius should be as large as is practicable, given the restriction on the internal layout of the building.

Acknowledgements

This study was supported by Australian Research Council awarded to K.C.S. Kwok and H.F. Rohde. The efforts of Mr. G. Arbuthnot in making models are acknowledged. The help of Ms. K. Pham in tracing graphs is also acknowledged.

References

1) Aachenbach, E., "Influence of Surface Roughness on the Cross-flow around a Circular Cylinder," *Journal of Fluid Mechanics,* Vol. 46, Part 2, pp. 321~335, 1971
2) Australian Standard 1170, Part 2-Wind Forces, "Minimum Load on Structures," Standard Association of Australia, 1989
3) Bearman, P. W., "The Flow around a Circular Cylinder in the Critical Reynolds Number Regime," NPL Aero. Rep. 1257, National Physical Lab., U. K. January, 1968
4) Best, R. J. and J. D. Holmes, "Model Study of Wind Pressures on an Isolated Single Storey House," James Cook University Wind Engineering Report 3/78, James Cook University of North Queensland, Australia, 1978
5) Charrett, D. E., P. H. Incoll, and N. Kozlovsky, "Modular Buildings for Antarctica," *First National Structural Conference,* Melbourne, August 26-28, pp. 586~591, 1987
6) Cheung, J. C. K. and W. H. Melbourne, "Turbulence Effects on Some Aerodynamec Parameters of a Circular Cylinder at Supercritical Reynolds Numbers," *Journal of Wind Engineering and Industrial Aerodynamics,* Vol. 14, pp. 399~410, 1983
7) Davonport, A. G., D. Surry, and T. Stathopoulos, "Wind Loads on Low Rise Buildings : Final Report of Phases I and II, BLWT-SS4-1977, The Univeristy of Western Ontario, London, Canada, 1977
8) Davonport, A. G., D. Surry, and T. Stathopoulos, "Wind Loads on Low Rise Buildings : Final Report on Phase III, BLWT-SS4-1978, The University of Western Ontario, London, Canada, 1978
9) Eaton, K. J. and J. R. Mayne, "The Measurement of Wind Pressures on Two Storey Hou-

ses at Aylesbury, *J. Ind. Aero. dyn.*, Vol. 1, pp. 67～109, 1975

10) Engineering Sciences Data Unit. "Characteristics of Atmospheric Turbulence near Ground, Part II : Single Point Data for Strong Winds (Neutral Atmosphere)" Data Item ESDU 74031, 1974

11) Engineering Sciences Data Unit. "Mean Forces, Pressure and Flow Field Velocities for Circular Cylindrical Structures : Single Cylinder with Two-Dimensional Flow," Item No. 80025, 1980

12) Farell, C., "Flow around Fixed Circular Cylinders : Fluctuating Loads," *Journal of Engineering Mechanics Division*, ASCE, Vol. 107, No. EM3, Proc. Paper 16330, June, pp. 565～558, 1981

13) Farell, C., "Flow around Fixed Circular Cylinders : Fluctuating Loads," Closure, *Journal of Engineering Mechanics Division*, ASCE, Vol. 109, No.4, August, 1983, pp. 1153～1156, 1983

14) Finnigan, J. J. and R. A. Longstaff, "A Wind Model Study of Forced Convective Heat Transfer from Cylindrical Grain Storage Bins," *Journal of Wind Engineering and Industrial Aerodynamics*, Vol. 10, pp. 191～211, 1982

15) Gosbell, K. and I. Holmes, "The Rebuilding of Australia's Antarctic Stations, *Antarctic Logistics Symposium*, Leningrad, June, Prepared by Department of Transport and Construction and Antarctic Division, Department of Science and Technology, 1982

16) Holmes, J. D., "Wind Pressures and Forces on Tropical Houses," Final Report of Project No. 17 of the Ausralian Housing Research Council, 1980

17) Holmes, J. D. and R. J. Best, "An Approach to the Determination of Wind Loads Effects on Low Rise Buildings," *J. Wind Eng. and Ind. Aerodyn.*, Vol. 7, pp. 273～287, 1981

18) Incoll, P., "The Influence of Architectural Theory on the Design of Australian Antarctic Stations," Australian Construction Services, July, 1990

19) Kim, D. H., K. C. S. Kwork, and H. F. Rohde, "Wind Tunnel Test of Wind Loads on Various Shapes of Elevated Buildings for Antarctic Use," Research Report No. 608, School of Civil and Mining Engineering, The University of Sydney, Australia, 1990

20) Kim, S. and K. C. Mehta, "Wind Loads on Flat Roof Area Through Full-scale Experiment," Institute for Disaster Research and Department of Civil Engineering, Texas Tech. University, Lubbock, Texas, 1977, 1977

21) Kwok, K. C. S., "Wind Tunnel Test Techniques," Seminar, Designing for Wind to AS 1170, Part 2, March, The Civil Panel, Sydney Division, The Institute of Engineers, Australia, 1985

22) Macdonald, B. E., "Wind Loads on Circular Cross-section Bins, Silos and Tanks," M. Eng. Thesis, School of Civil and Mining Engineering, University of Sydney, Australia, 1987

23) Marshall, R. D., "The Measurement of Wind Loads on a Full-scale Mobile Home," National Bureau of Standards, Washington D. C., NBWT－SS8－1977, The Univ. of Western Ontario, London, Canada, 1977

24) Mulhearn, R. J., H. J. Banks, J. J. Finnigan, and P. C. Annis, "Wind Forces and Their Influence on Gas Loss from Grain Storage Structures," Journal of Stored Product Research, Vol. 12, pp. 129～142, 1976

25) Radok, U., "Snow Drift," *J. Glaciol*, Vol. 19, No. 81., pp. 123～139, 1977

26) Roshko, A., "Experiments on the Flow Past a Circular Cylinder at Very High Reynolds Number," *Journal of Fluid Mechanics*, Vol. 78, part 3, 1961, pp. 561～576, 1961

27) Roy, R. J., "Wind Tunnel Measurements of Total Loads on a Mobile Home," *J. of Wind*

Eng. Struct., Vol. 6, pp. 119~135, 1983

28) Surry, D., T. Stathopoulos, A. G. Davenport, "Wind Loading on Low Rise Buildings," Canadian Structural Engineering Conference, 1978

29) Vickery, B. J., "Wind Loads on Low Rise Buildings," Seminar Paper, Darwin Reconstruction Commission, Darwin, 1976